

Evidence for mechanical softening-hardening dual anomaly in transition metals from shock-compressed vanadium

Hao Wang^{1,2,*}, J. Li^{1,*}, X. M. Zhou^{1,*}, Y. Tan¹, L. Hao¹, Y. Y. Yu¹, C. D. Dai¹, K. Jin¹, Q. Wu¹, Q. M. Jing¹, X. R. Chen^{2,†}, X. Z. Yan³, Y. X. Wang⁴, and Hua Y. Geng^{1,5,‡}

¹National Key Laboratory of Shock Wave and Detonation Physics, Institute of Fluid Physics, China Academy of Engineering Physics (CAEP), P.O. Box 919-102, Mianyang 621900, Sichuan, People's Republic of China

²College of Physics, Sichuan University, Chengdu 610065, People's Republic of China

³Jiangxi University of Science and Technology, Ganzhou 341000, Jiangxi, People's Republic of China

⁴College of Science, Xi'an University of Science and Technology, Xi'an 710054, People's Republic of China

⁵Center for Applied Physics and Technology, High Energy Density Physics Simulation (HEDPS), and College of Engineering, Peking University, Beijing 100871, People's Republic of China



(Received 31 August 2020; revised 23 August 2021; accepted 20 September 2021; published 5 October 2021)

Solids usually become harder and tougher under compression and turn softer at elevated temperature. Recently, the compression-induced softening and heating-induced hardening dual anomaly was predicted in group VB elements such as vanadium. Here, the evidence for this counterintuitive phenomenon is reported. By using accurate high-temperature, high-pressure (HP) sound velocities measured at Hugoniot states generated by shockwaves, together with first-principles calculations, we observe not only the prominent compression-induced sound velocity reduction but also strong heating-induced sound velocity enhancement in shocked vanadium. The former corresponds to the softening in the shear modulus by compression, whereas the latter reflects the reverse hardening by heat. These experiments also unveil another anomaly in Young's modulus. Based on the experimental and theoretical data, we infer that vanadium might transition from body-centered cubic into two different rhombohedral phases at ~ 79 and 116 GPa along the Hugoniot, respectively, which implies a dramatic difference in static and dynamic loading, as well as the significance of deviatoric stress and rate-relevant effects in HP phase transition dynamics.

DOI: [10.1103/PhysRevB.104.134102](https://doi.org/10.1103/PhysRevB.104.134102)

I. INTRODUCTION

Usually, compression increases not only the density but also the mechanical modulus and sound velocity. The larger the mechanical modulus of a material becomes, the more it can resist external deformation [1,2], a quality known as *hardening*. In contrast, increasing temperature often softens a material [3]. This phenomenon of compression-induced hardening and heating-induced softening (CIHHIS) is so general that it is considered as a golden rule in solid state physics, which had been well understood, and the variation in the modulus can be modeled accurately.

Recently, this rule was predicted to fail in vanadium (V) and niobium (Nb). Both elements were predicted to exhibit compression-induced softening (CIS) in shear modulus C_{44} . Niobium manifests multiple softening at high pressures (HPs), and a rhombohedral (RH) phase transition is induced in vanadium [4–7]. Another anomalous heating-induced hardening (HIH) in C_{44} of both V and Nb was also predicted at high temperature (HT). Therefore, a CISHIH dual anomaly was predicted in V and Nb; both have a striking magnitude and unusual nature. Nevertheless, direct experimental evidence is still absent.

On the other hand, Suzuki and Otani [6] and Landa *et al.* [7] once proposed the possibility of CIS on the phonon spectra of vanadium. This led to a hypothesis of concomitant structural transition driven by the soft mode. The first-order nature of these transitions was elucidated by Wang *et al.* [4,5], who also found that C_{44} of both V and Nb will increase at elevated temperature. Their work unequivocally demonstrated that the softening-hardening anomaly in mechanical moduli is more fundamental than the accompanying structural transitions.

In experiment, x-ray diffraction (XRD) with diamond anvil cell (DAC) was used to detect the hypothesized body-centered cubic (BCC)-to-RH transition in vanadium, in which the experimental transition pressure is still under debate [4,8,9]. The predicted reverse transition from RH back to BCC at HT was predicted by Wang *et al.* [4,5] and was then confirmed by recent XRD and laser-heating DAC experiments [10,11]. However, these static experiments detected only the RH1 phase [4,8–12]. The RH2 is still beyond the experimental scope. The observed BCC-RH1-BCC transition is just the manifestation of the anomaly in electronic structure rather than evidence for the softening-hardening phenomenon itself. Direct evidence for the predicted dual mechanical anomaly [4,5] is still required. It is crucial for understanding the properties of these metals at HP and HT.

In principle, the slope of acoustic phonon frequency at the long wavelength limit $\lim_{|k| \rightarrow 0} d\omega/dk$ can provide information about the elastic modulus and sound velocity. There have

*H.W., J.L., and X.M.Z. contributed equally to this work.

†xrchen@scu.edu.cn

‡s102genghy@caep.cn

been several attempts to measure the phonon dispersion at HP for Ta, Nb, and V [13,14], but the data quality is not accurate enough to derive useful elastic modulus or sound velocity. On the other hand, to measure the sound velocity directly by an ultrasonic method in the pressure range of interest of 50–150 GPa is very difficult.

Jing *et al.* [15,16] tried to measure the lattice deformation magnitude under nonhydrostatic compression conditions using XRD and DAC, and the yield strength of Nb and Ta were then derived. Their data indeed revealed some anomalous behavior. However, since this method requires the elastic modulus as an input, the results cannot tell anything about the elastic modulus itself.

On the other hand, dynamic experiments with shockwaves and fast diagnostic techniques can be used to measure the longitudinal sound velocity (C_l). It had been employed to probe the solid-solid transitions and shock melting in many metals [17–23]. In vanadium, in addition to the shock Hugoniot [24–26], the jump in C_l has been measured using transparent-window optical analyzer techniques to study the shock melting [27]. A similar method was also employed to detect the changes in yield strength [28]. Nevertheless, studies trying to probe the softening-hardening effect with dynamic experiments are lacking.

In this paper, a theoretical prediction of the CIS and HIH variation in the elastic modulus and sound velocity along the Hugoniot of vanadium is presented. It demonstrates how the dual anomaly manifests in dynamic shock conditions. Several

already available shockwave experiments were revisited to seek the possible signs of CISHIH as well as their deficiency. Two independent sets of shockwave experiments were then carried out. They confirm the predicted CISHIH dual anomaly in both the elastic modulus and sound velocity and serve as the experiment support in vanadium.

II. METHODS

A. Elastic constants

The elastic constants were calculated using the energy-strain method [29,30]. In general, the second elastic constants can be calculated based on the Euler strain (ε). In elastic theory, energy can be related to Euler strain through Taylor expansion in the form of strain tensor:

$$E = E_0 + V_0 \sum_i \sigma_i \varepsilon_i + \frac{1}{2!} V_0 \sum_{i,j=1}^6 C_{ij} \varepsilon_i \varepsilon_j + \dots \quad (1)$$

The coefficient of the Taylor expansion is the elastic constant that needs to be solved:

$$C_{ij} = \left. \frac{1}{V_0} \frac{\partial^2 E}{\partial \varepsilon_i \partial \varepsilon_j} \right|_{\varepsilon=0} \quad (2)$$

The polycrystalline moduli are calculated from the single-crystal elastic constants by using the Voigt-Reuss-Hill (VRH) method [31,32]:

$$9B_V = (C_{11} + C_{22} + C_{33}) + 2(C_{12} + C_{23} + C_{13}), \quad (3)$$

$$15G_V = (C_{11} + C_{22} + C_{33}) - (C_{12} + C_{23} + C_{13}) + 4(C_{44} + C_{55} + C_{66}), \quad (4)$$

$$B_R = \frac{1}{(S_{11} + S_{22} + S_{33}) + 2(S_{12} + S_{23} + S_{13})}, \quad (5)$$

$$G_R = \frac{15}{4(S_{11} + S_{22} + S_{33}) - 4(S_{12} + S_{23} + S_{13}) + 3(S_{44} + S_{55} + S_{66})}, \quad (6)$$

$$B_H = \frac{B_V + B_R}{2}, \quad G_H = \frac{G_V + G_R}{2}, \quad (7)$$

$$E_{VRH} = \frac{9B_{VRH}G_{VRH}}{3B_{VRH} + G_{VRH}}, \quad (8)$$

where $S_{ij} = [C_{ij}]^{-1}$, called the *compliance tensor*, in which the quantity with subscript H (Hill) is what we reported in this paper. The symbols of B , G , and E represent the bulk, shear, and Young's modulus, respectively.

In solids, since the compressional deformation and shear deformation of the materials have nonvanishing stiffness, there are corresponding compression (longitudinal) and shear (transverse) waves. Their velocity of propagation, namely, the sound velocity, is evaluated according to their definition, which depends on the elastic properties of the solid. For isotropic and homogeneous solids, the longitudinal and transverse sound velocities can be obtained as follows [33]:

$$C_l = \sqrt{\frac{B + \frac{4}{3}G}{\rho}}, \quad C_s = \sqrt{\frac{G}{\rho}}, \quad (9)$$

where ρ is the density, and B and G represent the bulk and shear modulus of the solid, respectively. In a three-dimensional solid, the sound velocity of a body (bulk sound velocity) can be understood as an average of longitudinal sound velocity and shear sound velocity as

$$C_b = \sqrt{C_l^2 - \frac{4}{3}C_s^2}. \quad (10)$$

B. Computational and experiment details

Theoretical calculation was carried out by using the VASP package based on density functional theory (DFT) [34,35]. A plane-wave basis set was employed with a kinetic energy cut-off of 900 eV. The electron-core interaction was described by a projector-augmented wave (PAW) pseudopotential [36]. The

pseudopotential contained 13 valence electrons (including $3s^2$, $3p^6$, $3d^3$, and $4s^2$ states). Meanwhile, under HP, we discuss that the core-core overlap effect produced by this pseudopotential has no effect on the calculation results. The details can be seen in the Supplemental Material (SM) [37] and Refs. [38,39]. The electronic exchange-correlation functional was set to the generalized gradient approximation as parameterized by Perdew, Berke, and Ernzerhof [40]. A Monkhorst-Pack (MP) grid with a size of $30 \times 30 \times 30$ ($24 \times 24 \times 24$) was adopted for K -point sampling of the BCC (RH) structure. The self-consistent field convergence tolerance was set as 10^{-8} eV per cell (0.001 eV/Å) for energy (force).

To disentangle the effect of compression and temperature, the elastic modulus and sound velocity of polycrystalline vanadium along both isotherm and Hugoniot paths were calculated. In the latter case, the experimental Hugoniot data of Ref. [41] were used to set up the corresponding thermodynamic conditions. The thermal electronic contribution was fully considered via the electronic free energy functional of finite temperature DFT of Mermin [42]. Because the temperature range we are concerned with is below the melting point, and previous studies have shown that, in this temperature range, the softening due to phonons (other than the corresponding thermal expansion contribution, which has been included in this paper automatically) is much smaller than the electronic part [4,43], we neglect this phonon contribution here to focus on the much more prominent electronic effects.

The shockwave sound velocity was measured using a two-stage gas gun [44]. The polycrystalline vanadium sample was purchased commercially with a purity of 99.9%. The sample thickness was 2.9 mm. For pressures < 117 GPa, the direct-reverse impact method [44,45] was employed. For higher pressures, a multiple-step method [46] with four steps was employed, with a step size of 0.5 mm. In all experiments, single-crystal [100] LiF was used as the optical window for the photonic Doppler velocimetry measurement. In this paper, we focus mainly on the physical implications of these experimental data. The technical details, experimental sample information, and data analysis of these experiments are presented in the SM [37] and Refs. [24,47].

III. RESULTS AND DISCUSSION

Our calculations confirm the previously predicted softening-hardening effect in single-crystalline vanadium C_{44} [4]. The data at 0 K are in good agreement with other theoretical work [7,12,48], as shown in the SM [37]. However, it is unclear whether this anomalous phenomenon is still perceptible in polycrystalline samples. To examine this, the elastic modulus of polycrystalline vanadium at HP and HT along different isotherms were calculated using the VRH average of single-crystalline elastic constants.

The results are shown in Fig. 1(a), in which both the bulk modulus (B) and sound velocity (C_b) do not exhibit perceptible softening or hardening. However, a strong CISHH is observed in the polycrystalline shear modulus (G) and Young's modulus (E) of vanadium [Figs. 1(b) and 1(c)]. The latter is in sharp contrast to the normally expected HIS behavior [49]. This softening-hardening effect modifies mainly the anisotropic components but still presents in polycrystalline

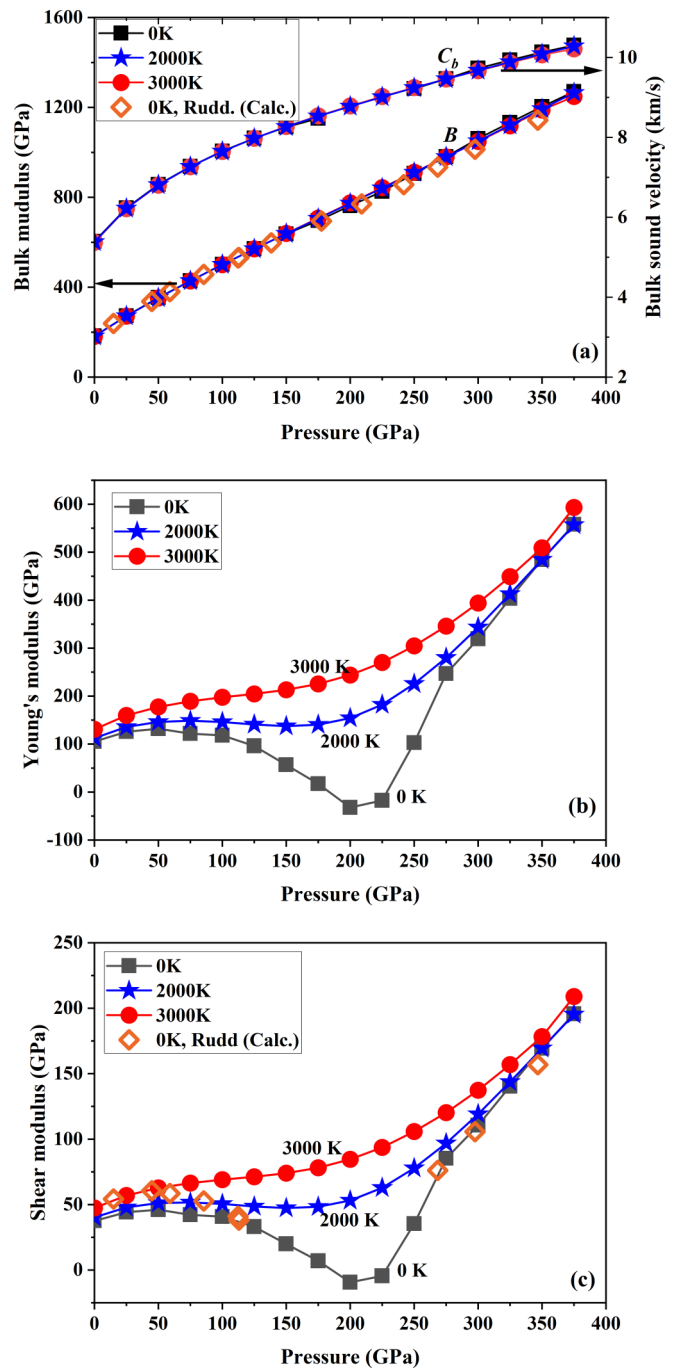


FIG. 1. Calculated high-pressure (HP) and high-temperature (HT) elastic constants of polycrystalline body-centered cubic (BCC) vanadium: (a) B and C_b , (b) E , and (c) G .

samples via the microscale anomalous single-crystal elastic response. The B and G reported by Rudd and Klepeis [49] are in good agreement with our data. The small deviation in Fig. 1(c) at low pressure is due to the difference between the plane-wave PAW and full-potential linear muffin-tin orbital method [7,50] and the different convergence criteria that were employed.

Here, we report the softening-hardening anomaly of E in Fig. 1(b). We find it stems from the slight CIS in C_{44} and C_{11} of single-crystalline vanadium [4,7,51]. Its direct implication

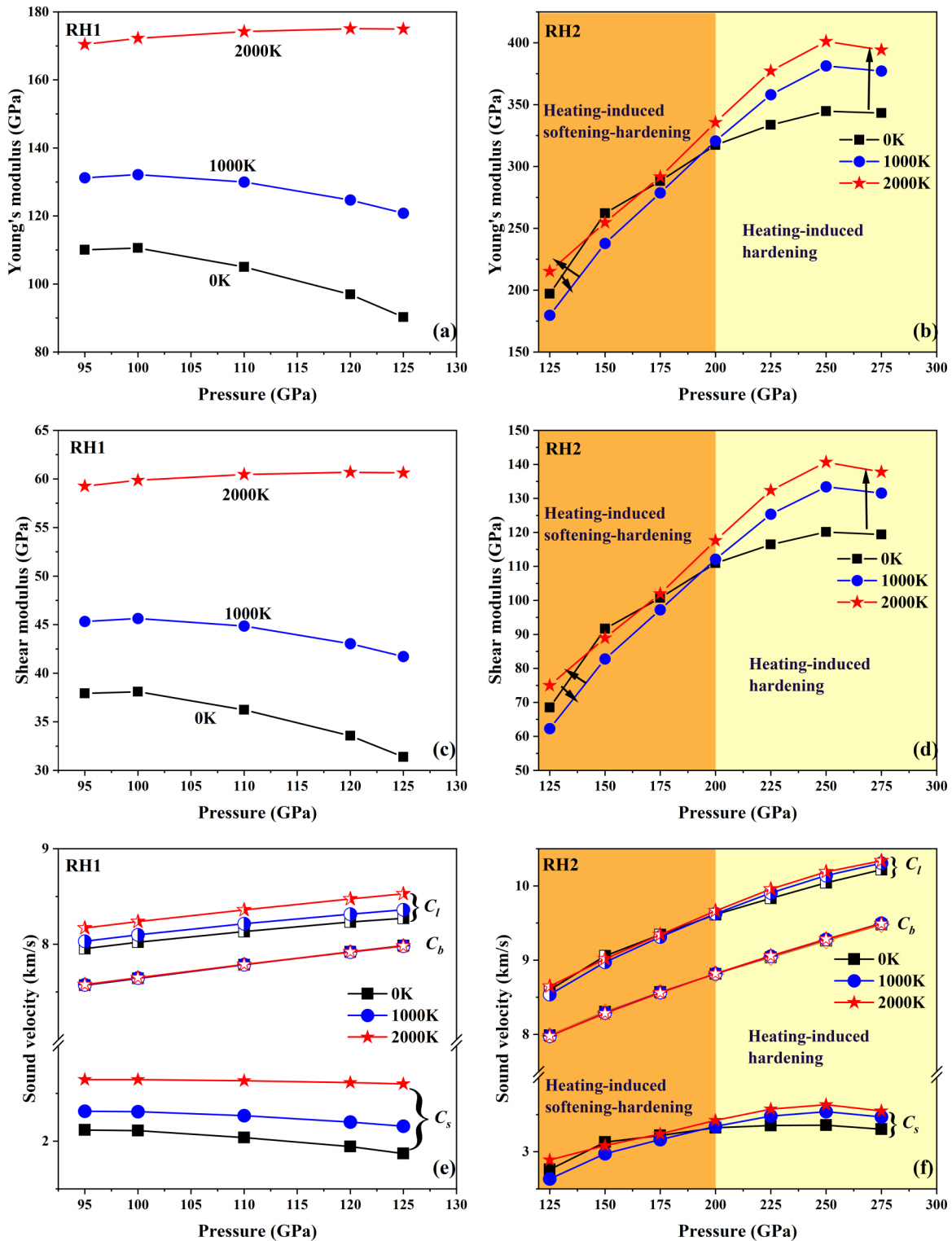


FIG. 2. Calculated variation of polycrystalline elastic constants and sound velocities of two different rhombohedral (RH1 and RH2) phases as a function of pressure at different temperatures, respectively. Notice the strong compression-induced softening and heating-induced hardening (CISHIH) in RH1 phase and the heating-induced softening to heating-induced hardening (HIS-HIH) crossover in RH2 phase (as indicated by the arrows). In both phases, bulk sound velocity C_b is almost temperature independent.

is that C_l should also exhibit a strong softening-hardening effect. This insight paves the way to utilize shockwave methods and polycrystalline samples to probe the evidence of CISHIH along the Hugoniot of vanadium. This kind of dynamic ex-

periment is usually easier to carry out than static HP-HT experiments.

On the other hand, both theory and experiment suggest that vanadium transforms into RH phases and then back to BCC at

HP [4–12]. This transition might alter the elastic constants and the corresponding sound velocity. Therefore, we also calculate the elastic modulus of polycrystalline RH phases and compare them with the BCC phase.

Figure 2 shows the polycrystalline elastic constants and sound velocity of RH1 and RH2 structures along isotherms, respectively. The calculation suggests that the bulk modulus of RH1 and RH2 are insensitive to temperature. It also should be noted that the bulk sound velocities of RH1 and RH2 are the same as that of BCC: all of them do not show any temperature dependence. The shear modulus in RH1 phase displays strong CIS and HIH [Fig. 2(c)]. In terms of the sound velocity, the effect of HIH becomes more obvious [Fig. 2(e)]. It should be noted that RH2 begins to show CIS at very HP (>250 GPa), whereas the shear modulus still has HIH when pressure is >200 GPa [Fig. 2(d)]. On the other hand, if the pressure is <175 GPa, the shear modulus of RH2 softens first and then hardens up with the increased temperature [namely, heating-induced softening-hardening, as the arrows in Fig. 2(d) indicate]. Of course, this situation mainly occurs when the temperature is low. As the temperature rises, RH2 still exhibits HIH. The Young's modulus [Fig. 2(b)] and longitudinal sound velocity [Fig. 2(f)] have similar behavior.

The predicted anomalous elastic modulus in BCC and RH phases implies that the softening-hardening effect might also be detectable in sound velocity. Our calculated sound velocities of C_b , C_l , and C_s in polycrystalline vanadium along different loading paths are shown in Fig. 3. The main discoveries are (1) C_b increases monotonically with pressure and is independent of temperature and structure; (2) C_l and C_s show CISHIH in both BCC and RH1 phases; (3) HIH also presents in the RH2 phase but is weaker; (4) BCC and RH phases have noticeable differences in their pressure dependence, which might be helpful for identifying the possible BCC \rightarrow RH1 \rightarrow RH2 transitions [4,12]; and (5) there is a CIS anomaly in the C_l of BCC at \sim 75 GPa.

The predicted softening up to \sim 100 GPa in C_s along the Hugoniot of the BCC phase [Fig. 3(b)] is striking. In addition, by comparing the isotherm with the Hugoniot line under the same pressure, both RH1 and RH2 have a larger C_s if the temperature is higher. This makes their shock Hugoniot intersect with any given isotherms. That is, at a given pressure, the Hugoniot state always has a faster C_s than the isotherm if the shock temperature is greater than the given isotherm, and vice versa, a distinctive signature of the HIH anomaly. The same conclusion holds for C_l in both BCC and RH phases.

The above analysis displays how the predicted softening-hardening effect will manifest in shock sound velocity and provides a theoretical baseline to compare with experiment. Moreover, as shown in Fig. 3(b), the C_s of both RH1 and RH2 along the Hugoniot depart from that of the BCC phase. It therefore might be an indicator for the possible BCC-RH transition along shock Hugoniot.

With these advanced theoretical understandings, we revisit the published experimental data [27,28]. Moreover, two independent sets of experiments were also carried out for the purpose of solidifying the support of the CISHIH dual anomaly further. The experimental data are listed in Table I for the first dataset. The second dataset that were conducted independently is listed in Table II. These two sets

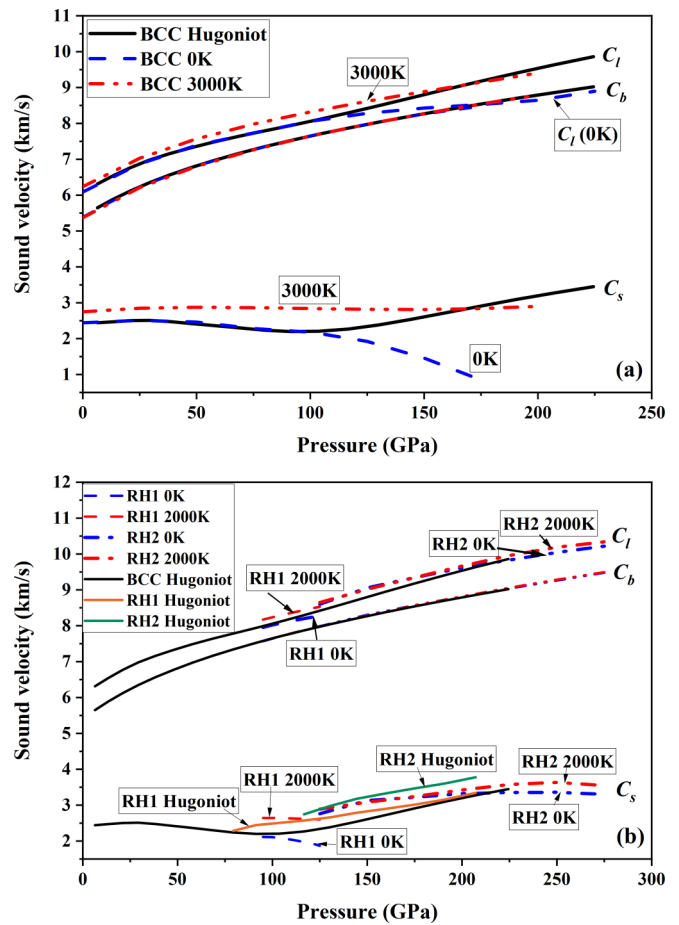


FIG. 3. Calculated high-pressure, high-temperature sound velocity of polycrystalline vanadium. (a) Comparison of Hugoniot with isotherms of 0 and 3000 K in body-centered cubic (BCC) phase. (b) Comparison of Hugoniot with isotherms of 0 and 2000 K in rhombohedral (RH) phases, along with the Hugoniot of the BCC phase.

of experiments were performed with different equipment and diagnostic devices for the purpose of accounting for the systematic uncertainty more appropriately, which was usually treated poorly in most experiments. The data of these four sets of shock experiments are shown in Fig. 4. It is evident that our theoretical data are in good agreement with the experimental data, especially for the BCC phase at low pressures.

As mentioned above, C_b is insensitive to temperature and structure. It therefore can be utilized as a standard reference to derive the experimental C_s from the directly measured C_l by using the relation $C_s^2 = 3(C_l^2 - C_b^2)/4$. The experimental C_s (half-filled points in Fig. 4) match our DFT results very well, even though it was discovered that DFT systematically underestimates G (as well as C_s) of vanadium at low pressures [51]. Some experimental data are slightly scattered, especially the point of Yu *et al.* [28] at 31.8 GPa. We scrutinized this datum and found that it is flawed. The inappropriate elastic-wave correction undermines it slightly. We also note that the datum at \sim 150 GPa of Dai *et al.* [27] departs significantly from all other points. Considering the obsolete technique employed by them, we rechecked the validity of this point by carrying out

TABLE I. Measured sound velocities of vanadium in direct-reverse impact (DRI) experiments. ρ_0 is the initial density of the flyer, h_f and W are the flyer thickness and velocity, u_w is the particle velocity at sample/window interface, t is the time duration of interface velocity plateau, and C_l is the Eulerian longitudinal sound velocity. The given uncertainties are the standard deviations.

| No. | ρ_0 (g/cm ³) | h_f (mm) | W (km/s) | t (ns) | u_w (km/s) | P_s (GPa) | C_l (km/s) |
|----------------|-------------------------------|---------------|-------------|----------|---------------|--------------|--------------|
| 1 ^a | 6.084 ± 0.023 | 2.920 ± 0.002 | 0.94 ± 0.01 | 905 ± 2 | 0.631 ± 0.006 | 9.99 ± 0.20 | 6.56 ± 0.13 |
| 2 | 6.084 ± 0.023 | 2.971 ± 0.002 | 2.89 ± 0.02 | 827 ± 2 | 1.886 ± 0.010 | 38.40 ± 0.80 | 7.06 ± 0.14 |
| 3 | 6.067 ± 0.023 | 2.946 ± 0.002 | 4.02 ± 0.02 | 742 ± 2 | 2.588 ± 0.014 | 59.07 ± 0.12 | 7.54 ± 0.15 |
| 4 | 6.104 ± 0.023 | 2.950 ± 0.002 | 4.71 ± 0.02 | 708 ± 6 | 3.012 ± 0.017 | 73.40 ± 0.15 | 7.68 ± 0.39 |
| 5 | 6.071 ± 0.023 | 2.962 ± 0.002 | 5.10 ± 0.03 | 682 ± 2 | 3.251 ± 0.018 | 81.89 ± 0.16 | 8.02 ± 0.16 |

^aElastic precursor wave correction was applied.

an experiment at almost the same pressure with a modern, advanced setup and diagnostic methods. The datum obtained at ~ 157 GPa, as shown in Fig. 4, is highly consistent with other data but is much lower than the original point of Dai *et al.* [27]. We therefore conclude that the point of Dai *et al.* [27] at ~ 150 GPa is invalid and will exclude it in the following analysis and discussion.

Clearly, the experimental C_s becomes smaller at higher shock pressures of up to ~ 100 GPa. Within this pressure range, the shock temperature is low, and its effect is insignificant, as shown in Fig. 4, which compares the shock Hugoniot with that of the BCC 0 K isotherm. The observed softening in C_s along the Hugoniot in Fig. 4 thus provides evidence for CIS in vanadium. This softening is more obvious when comparing the HP C_s with that of zero pressure, after considering the uncertainty and scattering of all relevant experimental data. On the other hand, the C_s of a normal metal usually becomes larger at HP, which is described well by the Steinberg-Guinan (SG) model [49,52]. The applicability of the original SG model to vanadium is discussed (see the SM [37] and Ref. [53]). The CIS anomaly becomes more striking if compared with this normally expected HP behavior.

To illustrate this more clearly and intuitively, we plotted the deviation of the experimental and theoretical shear sound

velocity with respect to the widely recognized SG model in Fig. 5(a). The shaded band in this figure contains all scattering and uncertainty of the experimental and theoretical data and represents an overall variation trend of the shear sound velocity along the shocking path. It is obvious that, when below a shock pressure of 100 GPa, not only the shear sound velocity at higher pressures becomes smaller than that of 0 GPa, but also its value continuously reduces with increasing pressure, and the deviation from the SG model at the same temperature becomes larger with the higher shock pressures. The largest softening takes place at ~ 75 GPa, with the shear sound velocity reduced by >0.5 km/s.

When beyond 100 GPa, the shock temperature effect becomes important, and HIH takes effect, as shown in Figs. 4 and 5(b). The calculated C_s of shock Hugoniot of the BCC phase departs from the 0 K isotherm at ~ 100 GPa, increasing to a higher value and intersecting the 3300 K isotherm at ~ 180 GPa. At this pressure, the experimental shear sound velocity is ~ 0.6 km/s faster than the 3000 K isotherm. The experimental C_s indeed follows this trend and continuously increases from ~ 75 to 200 GPa. Both our data and the experiment of Dai *et al.* [27] show a distinguishable departure from the 0 K isotherm of the BCC phase. The magnitude of the departure continues to increase with pressure and is larger than the experimental

TABLE II. Measured sound velocities of vanadium in DRI and multiple-step method (MSM) impact experiments. h_f and W are the flyer thickness and velocity, h_s is the sample thickness, u_w is the particle velocity at sample/window interface, t is the time duration of interface velocity plateau, C_l is the Eulerian longitudinal sound velocity, and R is the catchup ratio. The given uncertainties are the standard deviations.

| No. ^a | h_f (mm) | W (km/s) | h_s (mm) | t (ns) | R | u_w (km/s) | P_s (GPa) | C_l (km/s) |
|------------------|---------------|---------------|---------------|-----------|---------------|---------------|-------------|---------------|
| 1 | 0.919 ± 0.004 | 6.319 ± 0.032 | 1.018 ± 0.004 | 134.4 ± 6 | 4.365 ± 0.336 | 3.996 ± 0.040 | 173.0 ± 1.9 | 9.261 ± 0.364 |
| | | | 1.517 ± 0.004 | 112.4 ± 6 | | | | |
| | | | 2.027 ± 0.004 | 89.0 ± 6 | | | | |
| | | | 2.515 ± 0.004 | 67.5 ± 6 | | | | |
| 2 | 0.926 ± 0.004 | 5.924 ± 0.030 | 1.016 ± 0.004 | 138.9 ± 6 | 4.445 ± 0.356 | 3.762 ± 0.038 | 157.7 ± 1.7 | 9.106 ± 0.362 |
| | | | 1.514 ± 0.004 | 109.6 ± 6 | | | | |
| | | | 2.026 ± 0.004 | 94.1 ± 6 | | | | |
| 3 | 2.929 ± 0.004 | 6.498 ± 0.032 | — | 610.7 ± 6 | — | 4.123 ± 0.041 | 116.2 ± 2.1 | 8.481 ± 0.355 |
| | | | 1.211 ± 0.004 | 183.2 ± 6 | | | | |
| | | | 1.708 ± 0.004 | 155.7 ± 6 | | | | |
| 4 | 0.770 ± 0.004 | 6.398 ± 0.032 | — | — | 6.446 ± 0.474 | 4.311 ± 0.04 | 193.1 ± 1.4 | 9.744 ± 0.501 |
| | | | 2.224 ± 0.004 | 131.1 ± 6 | | | | |
| | | | 2.708 ± 0.004 | 111.2 ± 6 | | | | |

^aShots No. 1 and No. 2 were performed with vanadium flyer, and No. 4 was performed with tantalum flyer to achieve a higher pressure. Shot No. 3 was performed with direct-reverse impact setup.

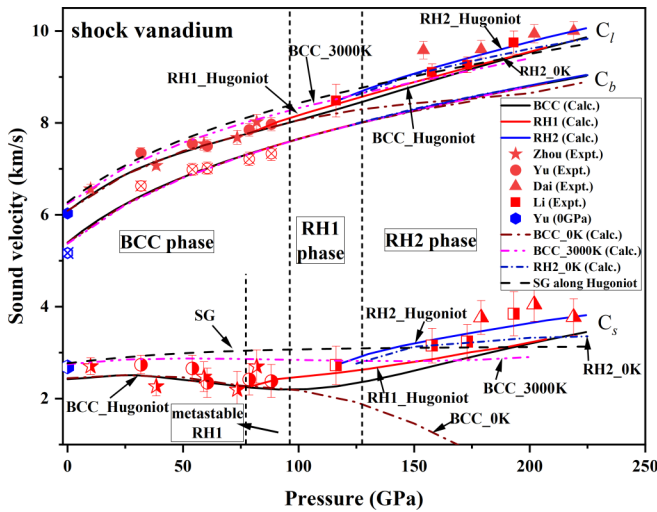


FIG. 4. Calculated and experimental sound velocity of shocked polycrystalline vanadium along the Hugoniot. The shock experimental data of Dai *et al.* [27], Yu *et al.* [28], and our two sets of experiments are shown (solid points for C_l , half-filled points for C_s). The open crossed points are for C_b as reported by Yu *et al.* [28]), respectively. The isothermal curve of the body-centered cubic (BCC) phase at 0 and 3000 K and that of rhombohedral 2 (RH2) at 0 K are also displayed for comparison. The Hugoniot sound velocity given by the Steinberg-Guinan (SG) model are also presented [49,52]. The phase boundaries at 0 K as estimated by Wang *et al.* [4] are given as vertical dotted lines.

uncertainty and the scattering of the data. They provide experimental support for an HIH anomaly in compressed vanadium; otherwise, the experimental C_s should be less than the 0 K isotherm of the BCC phase, which clearly is not the case. The same conclusion holds for C_l . Based on this observation, we infer that the C_l and C_s along an isentropic compression that is

accessible using a Z-machine or strong-laser technique should lie between the Hugoniot and those of the 300 K isotherm.

It should be pointed out that, though the experimental C_l and C_s show an interesting HIH phenomenon, having a larger slope of $\frac{dC_l}{dP}$ and $\frac{dC_s}{dP}$ along the Hugoniot than any isotherms when beyond 75 GPa, as shown in Fig. 4, the experimental data in fact do not match the BCC phase. This is in a sharp contrast to that for 0–75 GPa (in that range, the experimental C_l and C_s are in good agreement with the BCC phase). It is known that, in vanadium, a structural transition to RH takes place when compressed at room temperature. For comparison, the sound velocities of both RH1 and RH2 along the Hugoniot are calculated and displayed in Fig. 4. It is evident that the C_s and C_l of RH1 are in better agreement with the experimental data in the pressure range of 79–116 GPa, and the C_s and C_l of RH2 are in better agreement with the experimental data in the pressure range of 175–220 GPa.

We noticed that ~ 116 GPa, our experimental values are consistent with both RH1 and RH2 phases, and the theoretical calculation values of RH1 and RH2 have an intersection. Therefore, we infer that the transition pressure of RH1-RH2 of vanadium may be 116 GPa under shock loading. We also admit that more precise experimental measurements are needed to support our results within 116–175 GPa. We thus hypothesize that there might have been a BCC \rightarrow RH1 \rightarrow RH2 transition in shocked vanadium. The estimated transition pressures (P_t) are 79 GPa for BCC \rightarrow RH1 and 116 GPa for RH1 \rightarrow RH2.

The P_t of 79 GPa for BCC \rightarrow RH1 is close to the static DAC experimental result of Ding *et al.* [8] of 69 GPa. However, a P_t as low as 30 GPa was also reported [9], reflecting the challenge to address this problem experimentally. The discrepancies in the DAC experiments were largely attributed to nonhydrostatic conditions [9]. So far, the equilibrium phase diagram of compressed vanadium was calculated only for

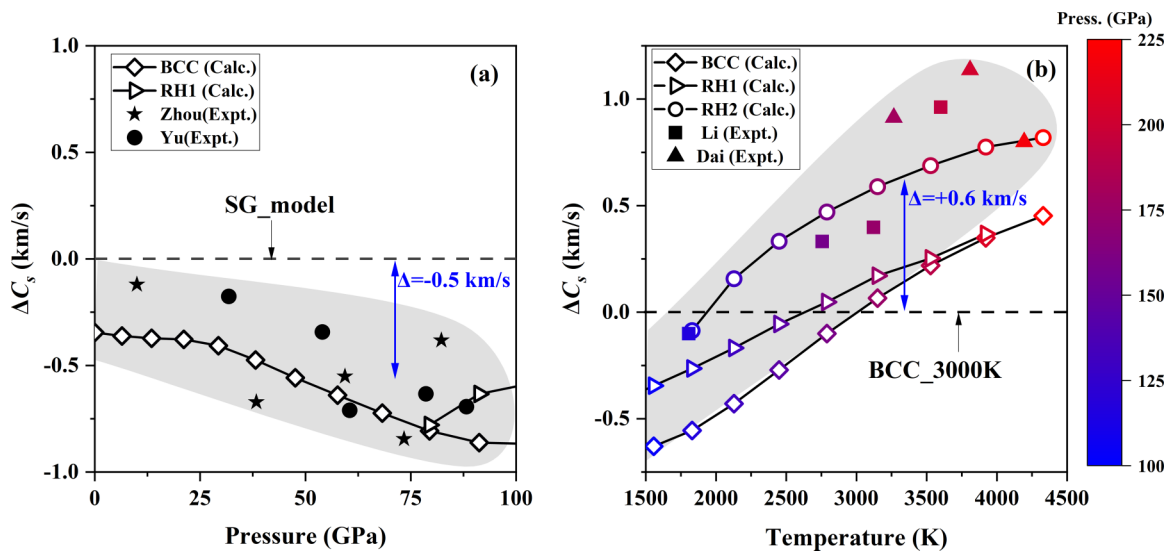


FIG. 5. Comparison of the shock experimental and theoretical shear sound velocity at high pressure and high temperature with respect to those values of (a) the Steinberg-Guinan (SG) model with the same temperature along the shock path, and (b) along the 3000 K isotherm of the body-centered cubic (BCC) phase at the same pressure. The shaded bands contain the scattering and uncertainty of the experimental data and represent an overall variation trend of the experimental data along the compression and heating path. The colormap in (b) indicates the shock pressure of each experimental or theoretical data.

hydrostatic conditions [4], and there was no attempt to consider deviatoric stress. In this sense, the equilibrium and hydrostatic DFT results might underestimate the stability of the RH phase if deviatoric stress is involved.

Dynamic shock compression always contains nonequilibrium and rate-dependent kinetic effects, which have not been included in any theoretical phase diagram. From the experimental data, we find that shocked vanadium has a sound velocity closer to RH phases rather than the BCC phase when >79 GPa. The occurrence of these HP phases, which are slight distortions of the BCC structure, could be due to the dynamic, nonequilibrium and nonhydrostatic nature of planar shockwaves. However, it should be pointed out that, as shown in Fig. 4, our first dataset of C_s is scattered slightly around the BCC Hugoniot and has large error bars when relative to the difference between the BCC and RH1 Hugoniot; our second dataset cannot unequivocally distinguish between BCC, RH1, and RH2 at 115 GPa or between RH1 and RH2 at 165 GPa. More accurate sound velocity data are required to pin down the exact P_r , even though our current experiments are compatible with the hypothetical shock-driven BCC-RH phase transitions.

IV. CONCLUSIONS

In summary, we predicted that the CISHIH dual anomaly in single-crystalline vanadium also presents in shocked polycrystalline vanadium. We also predicted an anomaly in both E and C_l . This theoretical insight paves the way to probing the softening-hardening anomaly in shockwave experiments directly. We then carried out two sets of shockwave sound velocity measurements. These data, together with previously reported experiments, provide evidence for a CIS anomaly up to ~ 75 GPa. The experiments also show significant HIH in shocked vanadium from 75 to 220 GPa, where both C_l and C_s along the Hugoniot increase much faster than any isotherms. These observations further improve the understanding of the CISHIH dual anomaly predicted in vanadium [4–7,12].

In addition, from the experimental and theoretical data, we also infer that shocked vanadium might experience a series

of structural transitions: the first one at 79 GPa for BCC \rightarrow RH1 and the second one at 116 GPa for RH1 \rightarrow RH2. These hypothesized transitions make vanadium harden further and are fully compatible with all available experimental data. This conclusion highlights the elusive and highly sensitive HP-HT behavior of the group VB metals under dynamic loading. Our findings could stimulate further theoretical and experimental research on this prominent CISHIH dual anomaly for practical applications. It also calls for more accurate experiments to prove or disprove the hypothesized BCC-RH transitions in shocked vanadium.

Note added in proof. Recent work by Stevenson *et al.* [54], suggests that in hydrostatic and equilibrium conditions, the high pressure RH phases of vanadium might indeed be a distortion of non-ideal BCC structure. This experimental signature is in line with previous theoretical assessment [51], and being compatible with the observed RH transitions under shock in this work induced by non-hydrostatic and non-equilibrium effects.

ACKNOWLEDGMENTS

This paper was supported by the National Natural Science Foundation Committee and China Academy of Engineering Physics (NSAF) under Grant No. U1730248 and No. U1830101, the National Natural Science Foundation of China under Grants No. 11672274, No. 11872056, No. 11904282, No. 11704163, and No. 11804131, the CAEP Research Project under Grant No. CX2019002, the Science Challenge Project TZ2016001, the China Postdoctoral Science Foundation under Grant No. 2017M623064, the Natural Science Foundation of Jiangxi Province of China under Grant No. 2018BAB211007. The simulation was performed on resources provided by the Center for Computational Materials Science at Tohoku University, Japan.

H.Y.G. conceived and designed the project. H.W. performed the calculations. X.M.Z., J.L., Y.T., and L.H. performed the experiments. All authors analyzed the data. H.Y.G. and H.W. wrote the draft. All authors contributed to revising the manuscript.

-
- [1] R. J. Hemley, H.-K. Mao, G. Shen, J. Badro, P. Gillet, M. Hanfland, and D. Häusermann, *Science* **276**, 1242 (1997).
 - [2] A. Krygier, P. D. Powell, J. M. McNaney, C. M. Huntington, S. T. Prisbrey, B. A. Remington, R. E. Rudd, D. C. Swift, C. E. Wehrenberg, A. Arsenlis, H. S. Park, P. Graham, E. Gumbrell, M. P. Hill, A. J. Comley, and S. D. Rothman, *Phys. Rev. Lett.* **123**, 205701 (2019).
 - [3] W. Li, H. Kou, X. Zhang, J. Ma, Y. Li, P. Geng, X. Wu, L. Chen, and D. Fang, *Mech. Mater.* **139**, 103194 (2019).
 - [4] Y. X. Wang, Q. Wu, X. R. Chen, and H. Y. Geng, *Sci. Rep.* **6**, 32419 (2016).
 - [5] Y. X. Wang, H. Y. Geng, Q. Wu, X. R. Chen, and Y. Sun, *J. Appl. Phys.* **122**, 235903 (2017).
 - [6] N. Suzuki and M. Otani, *J. Phys.: Condens. Matter* **14**, 10869 (2002).
 - [7] A. Landa, J. Klepeis, P. Söderlind, I. Naumov, O. Velikokhatnyi, L. Vitos, and A. Ruban, *J. Phys. Chem. Solids* **67**, 2056 (2006).
 - [8] Y. Ding, R. Ahuja, J. Shu, P. Chow, W. Luo, and H. K. Mao, *Phys. Rev. Lett.* **98**, 085502 (2007).
 - [9] Z. Jenei, H. P. Liermann, H. Cynn, J. H. P. Klepeis, B. J. Baer, and W. J. Evans, *Phys. Rev. B* **83**, 054101 (2011).
 - [10] D. Errandonea, S. G. MacLeod, L. Burakovsky, D. Santamaria-Perez, J. E. Proctor, H. Cynn, and M. Mezouar, *Phys. Rev. B* **100**, 094111 (2019).
 - [11] Y. Zhang, Y. Tan, H. Y. Geng, N. P. Salke, Z. Gao, J. Li, T. Sekine, Q. Wang, E. Greenberg, V. B. Prakapenka, and J.-F. Lin, *Phys. Rev. B* **102**, 214104 (2020).
 - [12] B. Lee, R. E. Rudd, J. E. Klepeis, and R. Becker, *Phys. Rev. B* **77**, 134105 (2008).

- [13] D. Antonangeli, D. L. Farber, A. Bosak, C. M. Aracne, D. G. Ruddle, and M. Krisch, *Sci. Rep.* **6**, 31887 (2016).
- [14] A. Bosak, M. Hoesch, D. Antonangeli, D. L. Farber, I. Fischer, and M. Krisch, *Phys. Rev. B* **78**, 020301(R) (2008).
- [15] Q.-M. Jing, Q. He, Y. Zhang, S.-R. Li, L. Liu, Q.-Y. Hou, H.-Y. Geng, Y. Bi, Y.-Y. Yu, and Q. Wu, *Chin. Phys. B* **27**, 106201 (2018).
- [16] Q. Jing, Q. Wu, J.-a. Xu, Y. Bi, L. Liu, S. Liu, Y. Zhang, and H. Geng, *J. Appl. Phys.* **117**, 055903 (2015).
- [17] L. M. Barker and R. E. Hollenbach, *J. Appl. Phys.* **45**, 4872 (1974).
- [18] D. H. Kalantar, J. F. Belak, G. W. Collins, J. D. Colvin, H. M. Davies, J. H. Eggert, T. C. Germann, J. Hawreliak, B. L. Holian, K. Kadau, P. S. Lomdahl, H. E. Lorenzana, M. A. Meyers, K. Rosolankova, M. S. Schneider, J. Sheppard, J. S. Stolken, and J. S. Wark, *Phys. Rev. Lett.* **95**, 075502 (2005).
- [19] C. Dai, J. Hu, and H. Tan, *J. Appl. Phys.* **106**, 043519 (2009).
- [20] M. C. Akin, J. H. Nguyen, M. A. Beckwith, R. Chau, W. P. Ambrose, O. V. Fat'yanov, P. D. Asimow, and N. C. Holmes, *J. Appl. Phys.* **125**, 145903 (2019).
- [21] J. H. Nguyen, M. C. Akin, R. Chau, D. E. Fratanduono, W. P. Ambrose, O. V. Fat'yanov, P. D. Asimow, and N. C. Holmes, *Phys. Rev. B* **89**, 174109 (2014).
- [22] J. M. Brown and R. G. McQueen, *J. Geophys. Res. Solid Earth* **91**, 7485 (1986).
- [23] R. S. Hixson and J. N. Fritz, *J. Appl. Phys.* **71**, 1721 (1992).
- [24] S. P. Marsh, in *LASL Shock Hugoniot Data* (University of California Press, Berkeley, 1980), p. 136, 296.
- [25] G. R. Gathers, *J. Appl. Phys.* **59**, 3291 (1986).
- [26] R. G. McQueen and S. P. Marsh, *J. Appl. Phys.* **31**, 1253 (1960).
- [27] C. Dai, X. Jin, X. Zhou, J. Liu, and J. Hu, *J. Phys. D: Appl. Phys.* **34**, 3064 (2001).
- [28] Y. Yu, Y. Tan, C. Dai, X. Li, Y. Li, Q. Wu, and H. Tan, *Appl. Phys. Lett.* **105**, 201910 (2014).
- [29] P. M. Marcus and S. L. Qiu, *J. Phys.: Condens. Matter* **21**, 115401 (2009).
- [30] Z.-J. Wu, E.-J. Zhao, H.-P. Xiang, X.-F. Hao, X.-J. Liu, and J. Meng, *Phys. Rev. B* **76**, 054115 (2007).
- [31] R. Hill, *Proc. Phys. Soc. A* **65**, 349 (1952).
- [32] A. Reuss, *Z. Angew. Math Mech.* **9**, 49 (1929).
- [33] K. D. Joshi, S. C. Gupta, and S. Banerjee, *J. Phys.: Condens. Matter* **21**, 415402 (2009).
- [34] G. Kresse and J. Furthmuller, *Comput. Mater. Sci.* **6**, 15 (1996).
- [35] G. Kresse and J. Furthmuller, *Phys. Rev. B* **54**, 11169 (1996).
- [36] P. E. Blöchl, *Phys. Rev. B* **50**, 17953 (1994).
- [37] See Supplemental Material at <http://link.aps.org/supplemental/10.1103/PhysRevB.104.134102> for experimental details, single-crystal elastic constants, SG model for elasticity, and the impact of core-core overlap of vanadium.
- [38] H. Y. Geng, H. X. Song, J. F. Li, and Q. Wu, *J. Appl. Phys.* **111**, 063510 (2012).
- [39] G. Kresse and D. Joubert, *Phys. Rev. B* **59**, 1758 (1999).
- [40] J. P. Perdew, K. Burke, and M. Ernzerhof, *Phys. Rev. Lett.* **77**, 3865 (1996).
- [41] M. V. Zhernokletov, V. N. Zubarev, R. F. Trunin, and V. E. Fortov, *Experimental Data on Shock Compressibility and Adiabatic Expansion of Condensed Matter at High Energy Density* (IPCP, Chernogolovka, 1996) (in Russian).
- [42] N. D. Mermin, *Phys. Rev.* **137**, A1441 (1965).
- [43] P. Keuter, D. Music, V. Schnabel, M. Stuer, and J. M. Schneider, *J. Phys.: Condens. Matter* **31**, 225402 (2019).
- [44] F. Xi, K. Jin, L. Cai, H. Geng, Y. Tan, and J. Li, *J. Appl. Phys.* **117**, 185901 (2015).
- [45] Y. Tan, Y. Yu, C. Dai, K. Jin, Q. Wang, J. Hu, and H. Tan, *J. Appl. Phys.* **113**, 093509 (2013).
- [46] F. Xi, K. Jin, H. Geng, Y. Li, Y. Tan, J. Li, Y. Zhang, L. Zhang, L. Cai, and Y. Sun, *AIP Adv.* **8**, 015023 (2018).
- [47] J. M. Brown and J. W. Shaner, in *Shock Waves in Condensed Matter—1983*, edited by J. R. Asay, R. A. Graham, and G. K. Straub (Elsevier, New York, 1984), p. 91.
- [48] L. Koči, Y. Ma, A. R. Oganov, P. Souvatzis, and R. Ahuja, *Phys. Rev. B* **77**, 214101 (2008).
- [49] R. E. Rudd and J. E. Klepeis, *J. Appl. Phys.* **104**, 093528 (2008).
- [50] K. H. Weyrich, *Phys. Rev. B* **37**, 10269 (1988).
- [51] Y. X. Wang, H. Y. Geng, Q. Wu, and X. R. Chen, *J. Chem. Phys.* **152**, 024118 (2020).
- [52] D. J. Steinberg, S. G. Cochran, and M. W. Guinan, *J. Appl. Phys.* **51**, 1498 (1980).
- [53] E. Walker, *Solid State Commun.* **28**, 587 (1978).
- [54] M. G. Stevenson, E. J. Pace, C. V. Storm, S. E. Finnegan, G. Garbarino, C. W. Wilson, D. McGonegle, S. G. Macleod, and M. I. McMahon, *Phys. Rev. B* **103**, 134103 (2021).